Contribution from the Department of Chemistry,
University of Victoria, P.O. Box 3055, Victoria, BC, Canada V8W 3P6

# Syntheses, Structure, and Reactivity of Cobalt and Nickel Complexes of 1,4,7-Trithiacyclodecane: Self-Exchange Rates for $Co(S_6)^{2+/3+}$ Couples from $^{59}Co$ NMR Spectroscopy

S. Chandrasekhar and A. McAuley*

*Received July 13, 1991*

Cobalt(II) and nickel(II) complexes of 1,4,7-trithiacyclododecane (**4**, [10]-ane$S_3$) have been synthesized and characterized by single-crystal X-ray diffraction and electronic and EPR spectroscopy. Both complexes contain the $[M(S_3)_2]^{2+}$ cation and crystallize in the monoclinic space group $P2_1/c$ (No. 14). Refinement of the species $Ni(4)_2(ClO_4)_2 \cdot 2CH_3NO_2$ ($a$ = 10.484 (4), $b$ = 15.272 (1), $c$ = 9.445 (1) Å; $\beta$ = 101.49 (1)°) converged at $R$ = 0.0705 ($R_w$ = 0.0738) for 199 parameters using 1848 reflections with $I > 2\sigma(I)$. Three S atoms from each ligand occupy a trigonal face in a distorted octahedral ion, where the average Ni–S bond length is 2.396 (7) Å. The cobalt complex is isomorphous with $a$ = 10.463 (3) Å, $b$ = 15.292 (4) Å, $c$ = 9.720 (2) Å, and $\beta$ = 102.16 (1)°. Refinement converged at $R$ = 0.0829 ($R_w$ = 0.0812) for 199 parameters using 1545 reflections with $I > 2\sigma(I)$. The Co–S distances all differ and cannot be distinguished as axial or equatorial bonds. $^{59}Co$ NMR signals show peaks at 2336 and 2268 ppm relative to $[Co(CN)_6]^{3-}$ owing to cis and trans isomers, respectively. By use of NMR line broadening in the presence of the corresponding cobalt(II) ion, the self-exchange electron-transfer rates for the $[Co(4)_2]^{3+/2+}$ ($4.3 \times 10^5$ $M^{-1}$ $s^{-1}$) and $[Co(1)_2]^{3+/2+}$ couples ($1.3 \times 10^5$ $M^{-1}$ $s^{-1}$) (**1** = 1,4,7-trithiacyclononane) have been determined. This is believed to be the first instance of such data being derived from this nucleus. Electrochemical data are consistent with the formation of M(III) and M(I) species, although for the latter in the case of nickel there is ESR evidence for a change in geometry.

## Introduction

Crown thioethers form a wide range of complexes with many transition-metal ions.[1-16] Transition-metal complexes of the nine-membered trithia macrocycle [9]-ane$S_3$ (**1**) (see Chart I) have been investigated extensively.[1,2,4-14,16-18] Homoleptic six-coordinate complexes of Fe(II), Fe(III), Co(II), Ni(II), Cu(II), Pd(II), Pt(II), Ag(I), Ru(II), and Rh(III) containing crown thioether ligands (e.g., [9]-ane$S_3$) have been isolated and characterized. These trithia systems provide examples of complexes where less common oxidation states may be stabilized.[16-18] Unlike the triaza ligand [9]-ane$N_3$ (**2**), the trithia ligand [9]-ane$S_3$ (**1**) forms low-spin complexes with Co(II).[19] Direct structural evidence for the donor–acceptor properties of crown thioethers have been provided recently by Blake et al.[20] in the complex [Fe-

Chart I

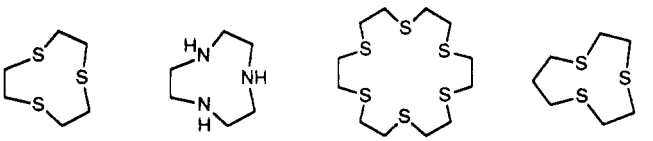


1 2 3 4

$([9]\text{-ane}S_3)_2](ClO_4)_3$. The spin-pairing energy is reduced, and low-spin Co(II) complexes are formed with [9]-ane$S_3$ and [18]-ane$S_6$ (**3**).[16,19,21] In an interesting study, Wieghardt and co-workers[22a] have analyzed the electron-transfer barriers in $Co(N_6)^{3+/2+}$ and $Co(S_6)^{3+/2+}$ couples in terms of the Marcus–Sutin model[23,24] for outer-sphere electron transfer. It is important that direct methods for determining electron self-exchange rates be used wherever possible to augment data derived from the Marcus cross correlation. The use of methods such as $^1H$ and $^{13}C$ NMR spectroscopy has been on the increase only in the recent past.[25-27]

In the present paper bis complexes of Co(II) and Co(III) with [10]-ane$S_3$ (**4**) have been synthesized and characterized by their electronic spectra, NMR spectra, and crystal structure.[28-30] The redox reactivity of the Ni(II) complexes has been investigated using EPR spectroscopy and cyclic voltammetry. Comparisons are made with the corresponding nine-membered-ring complexes. The $^{59}Co$ NMR spectra of the bis(thia)cobalt(III) complexes have been obtained and correlated with the electronic spectroscopic data. The rates of exchange in the electron-transfer reactions for the $[Co([10]\text{-ane}S_3)_2]^{3+/2+}$ and $[Co([9]\text{-ane}S_3)_2]^{3+/2+}$ couples have been measured for the first time using $^{59}Co$ NMR spectroscopy.

(1) Setzer, W. N.; Ogle, C. A.; Wilson, G. S.; Glass, R. S. *Inorg. Chem.* **1983**, *22*, 266.
(2) Wieghardt, K.; Kuppers, H.-J.; Weiss, H. Z. *Inorg. Chem.* **1985**, *24*, 3067.
(3) Corfield, P. W. R.; Ceccarelli, C.; Glick, M. D.; Moy, I. W.-Y.; Ochrymowycz, L. A.; Rorabacher, D. B. *J. Am. Chem. Soc.* **1985**, *107*, 2399.
(4) Wieghardt, K.; Kuppers, H.-J.; Raabe, E.; Kruger, C. *Angew. Chem., Int. Ed. Engl.* **1986**, *25*, 1101.
(5) Rawle, S. C.; Sewell, T. J.; Cooper, S. R. *Inorg. Chem.* **1987**, *26*, 3769.
(6) Bell, M. N.; Blake, A. J.; Gould, R. O.; Holder, A. J.; Hyde, T. I.; Lavery, A. J.; Reid, G.; Schroder, M. *J. Incl. Phenom.* **1987**, *5*, 169.
(7) Rawle, S. C.; Yagbasan, R.; Prout, K.; Cooper, S. R. *J. Am. Chem. Soc.* **1987**, *109*, 6181.
(8) Blake, A. J.; Gould, R. O.; Holder, A. J.; Hyde, T. I.; Lavery, A. J.; Odulate, M. O.; Schroder, M. *J. Chem. Soc., Chem. Commun.* **1987**, 118.
(9) Blake, A. J.; Holder, A. J.; Hyde, T. I.; Roberts, Y. V.; Lavery, A. J.; Schroder, M. *J. Organomet. Chem.* **1987**, *323*, 261.
(10) Rawle, S. C.; Cooper, S. R. *J. Chem. Soc., Chem. Commun.* **1987**, 308.
(11) Cooper, S. R.; Rawle, S. C.; Hartman, J. R.; Hintsa, E. J.; Adams, G. A. *Inorg. Chem.* **1988**, *27*, 1209.
(12) Blake, A. J.; Gould, R. O.; Holder, A. J.; Hyde, T. I.; Schroder, M. *J. Chem. Soc., Dalton Trans.* **1988**, 1861.
(13) Blower, P. J.; Clarkson, J. A.; Rawle, S. C.; Hartman, J. R.; Wolf, R. E., Jr.; Yagbasan, R.; Bott, S. G.; Cooper, S. R. *Inorg. Chem.* **1989**, *28*, 4040.
(14) Cooper, S. R. *Acc. Chem. Res.* **1988**, *21*, 141.
(15) Blake, A. J.; Holder, A. J.; Hyde, T. I.; Schroder, M. *J. Chem. Soc., Chem. Commun.* **1989**, 1433.
(16) de Groot, B.; Loeb, S. H. *Inorg. Chem.* **1990**, *29*, 4084.
(17) Blake, A. J.; Holder, A. J.; Hyde, T. I.; Schroder, M. *J. Chem. Soc., Chem. Commun.* **1987**, 987.
(18) Clarkson, J.; Yagbasan, R.; Blower, P. J.; Rawle, S. C.; Cooper, S. R. *J. Chem. Soc., Chem. Commun.* **1987**, 950.
(19) Wilson, G. S.; Swanson, D. D.; Glass, R. S. *Inorg. Chem.* **1986**, *25*, 3827.
(20) Blake, A. J.; Holder, A. J.; Hyde, T. I.; Schroder, M. *J. Chem. Soc., Chem. Commun.* **1989**, 1433.
(21) Hartman, J. R.; Hintsa, E. J.; Cooper, S. R. *J. Chem. Soc., Chem. Commun.* **1984**, 386.
(22) (a) Kuppers, H.-J.; Neves, A.; Pomp, C.; Wieghardt, K.; Nuber, B.; Weiss, J. *Inorg. Chem.* **1986**, *25*, 2400. (b) Wieghardt, K.; Kuppers, H.-J.; Steenken, S.; Nuber, B.; Weiss, J. *Z. Anorg. Allg. Chem.* **1989**, *573*, 43.
(23) Marcus, R. A. *Annu. Rev. Phys. Chem.* **1964**, *15*, 155.
(24) Sutin, N. *Prog. Inorg. Chem.* **1983**, *30*, 441.
(25) Smolenaers, P. J.; Beattie, J. K. *Inorg. Chem.* **1986**, *25*, 2259.
(26) Bernhard, P.; Sargeson, A. M. *Inorg. Chem.* **1988**, *27*, 2582.
(27) Dubbs, R. V.; Gahan, L. R.; Sargeson, A. M. *Inorg. Chem.* **1983**, *22*, 2523.
(28) Chandrasekhar, S.; McAuley, A. Presented at the 72nd Canadian Chemical Conference and Exhibition, Victoria, BC, Canada, June, 1989; Report 815.
(29) Chandrasekhar, S. Ph.D. Dissertation, University of Victoria, Victoria, BC, Canada, 1991.
(30) Setzer, W. N.; Cacioppo, E. L.; Guo, Q.; Grant, G. J.; Kim, D. D.; Hubbard, J. L.; VanDerveer, D. G. *Inorg. Chem.* **1990**, *29*, 2672.

0020-1669/92/1331-0480$03.00/0 

While this work was in progress, a paper was published on the synthesis and complexation of ten-membered-ring thioethers. In that study crystal structures of the Fe(II) complex and of a $Ni^{II}$(keto-10-ane$S_3$) species were presented.[31] The work described herein extends the data on these systems, especially in the area of redox chemistry.

## Experimental Section

All chemicals were of reagent grade except where otherwise indicated. Infrared spectra were obtained as KBr disks or as neat samples on NaCl plates with a Perkin-Elmer 283 grating spectrometer. High-field $^1H$ NMR and $^{13}C$ NMR spectra were obtained with a Bruker WM250 instrument or a Bruker 360 instrument. $^{59}Co$ NMR data were obtained on a Bruker 360 instrument. All chemical shifts are reported relative to tetramethylsilane except in the case of Co, where potassium hexacyanocobaltate(III) was used. Electronic spectra were recorded on a Cary-5 or a Philips PU 8740 spectrophotometer. EPR spectra were obtained with a Varian E6S spectrometer or a Bruker ER200tt spectrometer with an IBM/PC attachment. Diphenylpicrylhydrazyl radical (dpph) was used as a field marker ($g$ = 2.0037).

Elemental analyses were performed by Microanalytical Services, Vancouver, BC, Canada. Electrochemical measurements were recorded with a Princeton Applied Research Model 273 potentiostat–galvanostat, interfaced with an IBM/PC. Cyclic voltammograms were run using the "Headstart" program (Princeton). The electrochemical cell employed the standard three-electrode configuration, a platinum working electrode, a Pt-wire auxiliary electrode, and the reference electrode. In aqueous solutions the reference electrode was a Ag/AgCl electrode linked to the cell via a bridge containing saturated KCl, and 0.1 M NaCl was used as a supporting electrolyte. A silver wire was used as a reference electrode in nonaqueous systems containing 0.1 M $NEt_4BF_4$. Blank electrolyte solutions were scanned before each experiment and each time the ferrocenium/ferrocene couple ($Fc^+$/Fc) was used as an external standard to calibrate the reference electrode, $E_{1/2}(Fc^+/Fc)$ = 0.30 V vs the silver wire. All potentials are reported against the $Fc^+$/Fc standard couple ($E_{1/2}$ of $Fc^+$/Fc vs NHE = 0.40 V) and were found to be internally consistent. Acetonitrile was distilled over $CaH_2$ prior to use for electrochemical purposes.

The kinetics of electron-transfer reactions were studied by NMR line-broadening techniques. Stock solutions for the cobalt complexes of cobalt(II) complex were prepared and appropriate amounts of cobalt(III) species added in a 10-mm NMR tube to a final volume of 1.5 mL. The temperature was controlled to 25 ± 1 °C.

**Synthesis.** The ligand [10]-ane$S_3$ was synthesized by the methods based on previously published procedures of Buter and Kellogg[31] and Blower and Cooper.[32] The experimental details have been described earlier.[29]

*Caution!* Transition-metal perchlorates, especially with thioether ligands, are extremely hazardous and must be handled with great care. Only small amounts of materials should be prepared.

**[Co([10]-ane$S_3$)$_2$](ClO$_4$)$_2$.** A methanolic solution of $Co(ClO_4)_2 \cdot 6H_2O$, 143 mg (0.39 mmol), was added to a solution of the ligand [10]-ane$S_3$ (**4**), 164 mg (0.85 mmol) in 20 mL of methanol. The solution was refluxed for 5 h under a dinitrogen atmosphere and then filtered while hot. The filtrate was taken to dryness, and the residue was dissolved in $CH_3CN$ containing $NaClO_4$. Slow diffusion of ether yielded reddish brown needle-shaped crystals of the complex. Yield: 150 mg; 60%. Anal. Calcd for $C_{14}H_{28}S_6CoCl_2O_8$: C, 26.00; H, 4.36. Found: C, 26.01; H, 4.25.

**[Co([10]-ane$S_3$)$_2$](ClO$_4$)$_3$.** An aqueous solution of $Na_2S_2O_8$ (3 mL) was added to 27 mg of [Co([10]-ane$S_3$)$_2$](ClO$_4$)$_2$ in 2 mL of $H_2O$. The color changed from red to orange. Addition of a saturated solution of $NaClO_4$ (1 mL) initiated the precipitation of orange-yellow crystals, which were filtered off, washed with ethanol, and dried under vacuum. Yield: 28 mg; 90%. Anal. Calcd for $C_{14}H_{28}S_6CoCl_3O_{12}$: C, 22.53; H, 3.78. Found: C, 22.28; H, 3.66.

**[Ni([10]-ane$S_3$)$_2$](ClO$_4$)$_2$.** A solution of $Ni(ClO_4)_2 \cdot 6H_2O$, 183 mg (0.5 mmol), in ethanol (10 mL) was added dropwise to a solution of the ligand [10]-ane$S_3$ (**4**), 230 mg (1.18 mmol) in 10 mL of ethanol. The solution was refluxed for 0.5 h. The pink complex that precipitated out was filtered and recrystallized from acetonitrile solution of the complex by diffusion of ether. Yield: 0.23 g; 71%. Anal. Calcd for $C_{14}H_{28}NiCl_2O_8$: C, 26.01; H, 4.36; S, 29.76. Found: C, 25.92; H, 4.45; S, 29.34.

**[Ni([9]-ane$S_3$)$_2$](ClO$_4$)$_2$.**[1] This complex was prepared in a manner analogous to that for [Ni([10]-ane$S_3$)$_2$](ClO$_4$)$_2$ using the ligand [9]-ane$S_3$ (**1**). A purple crystalline solid of the perchlorate salt was obtained.

(31) Buter, J.; Kellogg, M. *Org. Synth.* **1987**, *65*, 150.
(32) Blower, P. J.; Cooper, S. R. *Inorg. Chem.* **1987**, *26*, 2009.

**Table I.** Experimental Crystallographic Data

| | | |
|---|---|---|
| formula | $NiC_{16}H_{34}S_6N_2Cl_2O_{12}$ | $CoC_{16}H_{34}S_6N_2Cl_2O_{12}$ |
| MW | 768.42 | 768.65 |
| space group | $P2_1$ (No. 14) | $P2_1/c$ (No. 14) |
| cell params | | |
| $a$, Å | 10.484 (4) | 10.463 (3) |
| $b$, Å | 15.272 (1) | 15.292 (4) |
| $c$, Å | 9.445 (0) | 9.720 (2) |
| $\alpha$, deg | 90 | 90 |
| $\beta$, deg | 101.49 (1) | 102.16 (1) |
| $\gamma$, deg | 90 | 90 |
| $V$, Å$^3$ | 1533.68 | 1520.30 |
| $Z$ | 2 | 2 |
| $D_{calc}$, g/cm$^3$ | 1.664 | 1.679 |
| $D_{measd}$, g/cm$^3$ | 1.674 | 1.677 |
| radiation (λ, Å) | Mo Kα (0.710 69) | Mo Kα (0.710 69) |
| $T$, °C | 22 ± 2 | 22 ± 2 |
| $\mu$, cm$^{-1}$ | 11.81 | 11.19 |
| $R$ | 0.0705 | 0.0829 |
| $R_w$ | 0.0738 | 0.0812 |

**Crystal Structure of [Ni([10]-ane$S_3$)$_2$](ClO$_4$)$_2$·2CH$_3$NO$_2$.** Pink crystals of the Ni complex were obtained by ether diffusion into a solution of the complex in nitromethane. The crystal with appropriate dimensions, 0.46 × 0.24 × 0.26 mm$^3$, was mounted in a Lindemann tube and Weissenberg and precession photography undertaken to establish the unit cell dimensions and the space group. The cell constants were refined on a Nonius CAD4 diffractometer using 25 centered reflections in the range $2\theta$ = 24–37°. Absorption corrections were made using the EMPABS (Nonius) program. The crystal data are given in Table I. Intensity measurements were carried out in the $\omega$–$2\theta$ scan mode with Zr-filtered Mo radiation, λ = 0.710 69 Å. A total of 2513 independent reflections were measured from which 1848 [$I > 2\sigma(I)$] were used after suppression.

The solution of the phase problem was achieved using MULTAN,[33] and the structure was completed by difference electron density maps and refined by the method of least squares. The atomic scattering factors used were those included in the SHELX-76 program[34] together with the Ni $f$ curve.[35] All the non-hydrogen atoms were refined anisotropically. The final refinement converged to $R$ = 0.0705 and $R_w$ = 0.0738 with a maximum shift/esd of 0.079 on the final cycle. A final difference map had a maximum peak of 0.71 e Å$^{-3}$.

**Crystal Structure of [Co([10]-ane$S_3$)$_2$](ClO$_4$)$_2$·2CH$_3$NO$_2$.** Dark brown crystals of diffraction quality were grown by vapor diffusion of diethyl ether into nitromethane solutions of the complex. Preliminary photography using Weissenberg and precession methods were carried out to establish the unit cell dimensions and the space group. The crystal was found to be isomorphous with the [Ni([10]-ane$S_3$)$_2$](ClO$_4$)$_2$·2CH$_3$NO$_2$ crystal. The cell constants were refined on a Nonius CAD4 diffractometer using 25 centered reflections in the range $2\theta$ = 16–36°. Absorption corrections were made as previously indicated. The crystal data are given in Table I. A total of 2407 reflections were measured out of which 1545, $I > 2\sigma(I)$, were used after suppression.

The coordinates for the Co atom and the three S atoms were used from that of the isomorphous Ni complex. The atomic scattering factors used were those included in the SHELX-76 program[36] together with the Co $f$ curve.[35] All non-hydrogen atoms were refined anisotropically. The final refinement converged to $R$ = 0.0829 and $R_w$ = 0.0812 with a maximum shift/esd of 0.073 on the final cycle. A final difference map had a maximum peak of 0.63 e Å$^{-3}$.

## Results

The transition-metal complexes Co(II/III) and Ni(II) with [10]-ane$S_3$ (**4**) were synthesized and characterized by X-ray crystallography and UV–visible, NMR, and ESR spectroscopies where applicable. The orange crystalline cobalt(III) complex was obtained by $S_2O_8^{2-}$ oxidation of the cobalt(II) species. Stable octahedral complexes with two trithia ligands were formed as a result of the endodentate conformation of the ligand in these complexes. The ligand field parameters and the redox properties of the complexes based on the trithia ligand were compared with those of the triaza analogues. Electrochemical studies provide

(33) Main, P. MULTAN. University of York, York, U.K., 1978.
(34) Sheldrick, G. M. SHELX76, Program for Crystal Structure Refinement. University of Cambridge, U.K., 1974.
(35) *International Tables for X-ray Crystallography*; Kynoch Press: Birmingham, U.K., 1974; Vol. IV.
(36) Cooper, S. R.; Rawle, S. C.; Hartman, J. R.; Hintsa, E. J.; Adams, G. A. *Inorg. Chem.* **1988**, *27*, 1209.

**Table II.** Fractional Atomic Coordinates and Temperature Parameters for $[Ni([10]\text{-}aneS_3)_2](ClO_4)_2 \cdot 2CH_3NO_2$[a]

| atom | x/a | y/b | z/c | $U_{eq}$,[b] Å$^2$ |
|---|---|---|---|---|
| Ni(1) | 0 (0) | 0 (0) | 0 (0) | 383 (4) |
| S(1) | -2118 (20) | 3520 (14) | 23399 (22) | 530 (7) |
| S(2) | 8989 (24) | 14312 (14) | -1480 (24) | 605 (8) |
| S(3) | 20609 (22) | -6643 (15) | 8775 (23) | 627 (8) |
| Cl(1) | 34984 (20) | 40070 (15) | 13151 (22) | 582 (7) |
| O(1) | 2227 (10) | 3804 (8) | 1368 (12) | 159 (2) |
| O(2) | 3680 (13) | 3863 (12) | 1 (11) | 200 (3) |
| O(3) | 3654 (15) | 4893 (8) | 1628 (20) | 246 (3) |
| O(4) | 4343 (14) | 3600 (10) | 2205 (15) | 228 (3) |
| C(1) | 745 (9) | 1360 (5) | 2696 (9) | 61 (2) |
| C(2) | 526 (9) | 1955 (6) | 1372 (10) | 66 (2) |
| C(3) | 2666 (3) | 1518 (9) | 42 (14) | 89 (2) |
| C(4) | 3447 (14) | 867 (7) | 1011 (14) | 111 (3) |
| C(5) | 3344 (14) | -19 (8) | 333 (19) | 130 (3) |
| C(6) | 2155 (10) | -600 (11) | 2765 (3) | 90 (3) |
| C(7) | 918 (8) | -458 (6) | 3285 (10) | 66 (2) |
| C(8) | 5937 (10) | 1953 (8) | 3795 (11) | 83 (2) |
| N(1) | 7085 (10) | 1955 (6) | 3149 (11) | 90 (2) |
| O(5) | 8146 (10) | 1948 (7) | 4014 (13) | 149 (2) |
| O(6) | 6970 (14) | 1935 (9) | 1981 (11) | 204 (3) |
| C(3′) | 625 (23) | -342 (14) | 3766 (15) | 45 (4)′ |
| C(4′) | 1509 (20) | -963 (15) | 3214 (26) | 52 (4)′ |
| C(5′) | 2633 (21) | -522 (18) | 2759 (4) | 41 (4)′ |
| C(6′) | 3250 (16) | 147 (11) | 550 (24) | 31 (4)′ |
| C(7′) | 2564 (12) | 1012 (20) | 317 (46) | 635 (5)′ |

[a] Estimated standard deviations are given in parentheses. Coordinates × $10^n$, where $n$ = 5, 5, 4, 4, and 4 for S, Cl, O, C, and N. Temperature parameters × $10^n$, where $n$ = 4, 4, 4, 3, 3, and 3 for Ni, S, Cl, O, C, N. [b] $U_{eq}$ = the equivalent isotropic temperature parameter. $U_{eq} = {}^1/_3\sum_i\sum_j U_{ij}a_i^*a_j^*(a_ia_j)$. Primed values indicate that $U_{iso}$ is given. $T = \exp[-(8\pi^2U_{iso}(\sin^2\theta)/\lambda^2)]$. Disorder occupancy for C3, C4, C5, C6, and C7 = 74%.

**Table III.** Selected Bond Lengths (Å) and Bond Angles (deg) for $[Ni([10]\text{-}aneS_3)_2](ClO_4)_2 \cdot 2CH_3NO_2$[a]

| | | | |
|---|---|---|---|
| S(1)-Ni(1) | 2.403 (2) | S(2)-Ni(1) | 2.396 (2) |
| S(3)-Ni(1) | 2.386 (2) | C(1)-S(1) | 1.832 (8) |
| C(7)-S(1) | 1.830 (1) | C(3′)-S(1) | 1.830 (1) |
| C(2)-S(2) | 1.798 (9) | C(3)-S(2) | 1.829 (1) |
| C(7′)-S(2) | 1.830 (1) | C(5)-S(3) | 1.830 (1) |
| C(6)-S(3) | 1.831 (1) | C(5′)-S(3) | 1.830 (1) |
| C(6′)-S(3) | 1.830 (1) | | |
| S(2)-Ni(1)-S(1) | 88.0 (1) | S(3)-Ni(1)-S(2) | 94.1 (1) |
| S(3)-Ni(1)-S(1) | 90.1 (1) | | |

[a] Estimated standard deviations are given in parentheses.

evidence for Co(I), Ni(I), and Ni(III) oxidation states. The self-exchange rate constants for the electron-transfer reactions of the $[Co(\mathbf{4})_2]^{3+/2+}$ and $[Co(\mathbf{1})_2]^{3+/2+}$ couples have been obtained directly for the first time using $^{59}Co$ NMR spectroscopy.

## Discussion

**Crystal Structures.** The molecular structure of the Ni complex with the atomic labeling scheme is shown in Figure 1, while the fractional atomic coordinates, bond lengths, and bond angles are contained in Tables II and III. The asymmetric unit consists of a half-molecule of the complex cation with one perchlorate anion and one molecule of nitromethane. The Ni atom occupies an inversion center, and the other half of the complex cation was obtained by inversion at this center. The Ni atom is coordinated to six S atoms, three from each ligand occupying a trigonal face, thus forming a distorted octahedral complex.

The average Ni–S bond length was 2.396 (7) Å (mean of 3) and compares well with the $[Ni([9]\text{-}aneS_3)_2]^{2+}$ complex[1] (2.386 (14) Å). The rest of the bond lengths fall in the normal ranges as expected, except C(3)–C(4) (1.336 (18) Å), C(4)–C(5) (1.395 (18) Å), and C(6)–C(7) (1.726 (18) Å). This may be due to disorder of the C(3)–C(4)–C(5) part of the ring. The carbon atoms in the propyl ring (C(3), C(4), C(5)) and the ethyl ring (C(6), C(7)) were disordered, and the site occupation factors for these carbon atoms were varied to model the positional disorder.

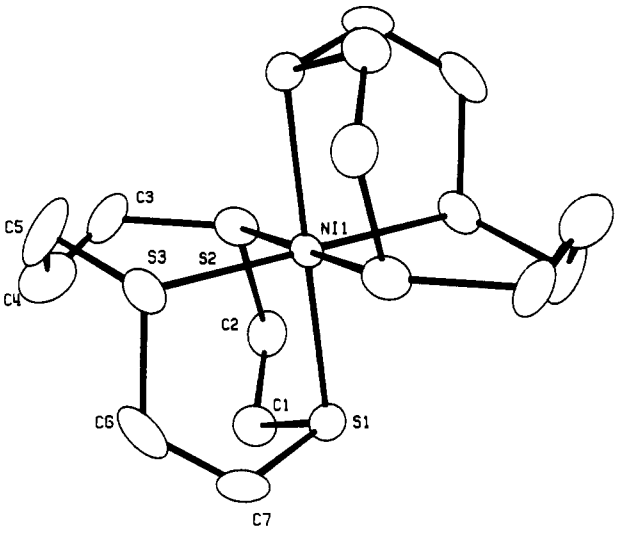


**Figure 1.** ORTEP diagram of $[Ni(\mathbf{4})_2](ClO_4)_2$ with 25% thermal ellipsoids.

**Table IV.** Fractional Atomic Coordinates and Temperature Parameters for $[Co([10]\text{-}aneS_3)_2](ClO_4)_2 \cdot 2CH_3NO_2$[a]

| atom | x/a | y/b | z/c | $U_{eq}$,[b] Å$^2$ |
|---|---|---|---|---|
| Co(1) | 0 (0) | 0 (0) | 0 (0) | 420 (6) |
| S(1) | -2184 (27) | 3507 (21) | 22612 (30) | 659 (11) |
| S(2) | 8948 (32) | 14296 (20) | -1532 (33) | 727 (12) |
| S(3) | 19592 (28) | -6339 (20) | 8250 (29) | 665 (11) |
| Cl(1) | 35238 (27) | 40092 (21) | 13331 (29) | 654 (10) |
| O(1) | 2254 (12) | 3815 (10) | 1389 (15) | 168 (3) |
| O(2) | 3679 (15) | 3869 (14) | 20 (14) | 214 (3) |
| O(3) | 3679 (19) | 4872 (12) | 1704 (23) | 273 (4) |
| O(4) | 4363 (16) | 3596 (12) | 2239 (17) | 237 (3) |
| C(1) | 746 (12) | 1361 (7) | 2695 (12) | 72 (3) |
| C(2) | 557 (12) | 1964 (7) | 1393 (13) | 75 (3) |
| C(3) | 2669 (4) | 1532 (12) | 72 (19) | 111 (3) |
| C(4) | 3457 (18) | 849 (9) | 989 (18) | 114 (3) |
| C(5) | 3300 (15) | -36 (9) | 311 (21) | 107 (3) |
| C(6) | 2180 (12) | -570 (14) | 2741 (3) | 86 (3) |
| C(7) | 931 (11) | -443 (8) | 3244 (12) | 75 (3) |
| C(8) | 5893 (13) | 1941 (10) | 3786 (14) | 93 (3) |
| N(1) | 7034 (13) | 1955 (7) | 3116 (15) | 104 (3) |
| O(5) | 8120 (13) | 1937 (8) | 4019 (17) | 165 (3) |
| O(6) | 6900 (18) | 1919 (11) | 1952 (15) | 233 (3) |
| C(3′) | 566 (29) | -336 (18) | 3742 (20) | 50 (5)′ |
| C(4′) | 1541 (28) | -915 (23) | 3256 (38) | 82 (6)′ |
| C(5′) | 2688 (27) | -583 (29) | 2708 (7) | 63 (6)′ |
| C(6′) | 3155 (21) | 181 (15) | 531 (32) | 36 (5)′ |
| C(7′) | 2606 (11) | 1090 (22) | 358 (52) | 177 (6)′ |

[a] Estimated standard deviations are given in parentheses. Coordinates × $10^n$ where $n$ = 5, 5, 4, 4, and 4 for S, Cl, O, C, and N. Temperature parameters × $10^n$, where $n$ = 4, 4, 4, 3, 3, and 3 for Co, S, Cl, O, C, and N. [b] $U_{eq}$ = the equivalent isotropic temperature parameter. $U_{eq} = {}^1/_3\sum_i\sum_j U_{ij}a_i^*a_j^*(a_ia_j)$. Primed values indicate that $U_{iso}$ is given. $T = \exp[-(8\pi^2U_{iso}(\sin^2\theta)/\lambda^2)]$. Disorder occupancy for C3, C4, C5, C6, and C7 = 73%.

The structure obtained is that of a meso stereoisomer in which the trimethylene bridges are trans to one another. For the $[Ni([12]\text{-}aneS_3)_2](BF_4)_2$ complex, one of the C–C single-bond lengths was found to be 1.30 (2) Å, also due to disorder in that part of the ring.[36]

The mean five-membered chelate bite angle was found to be 89.2 (11)° similar to that found in the $[Ni([9]\text{-}aneS_3)_2]^{2+}$ complex (88.5 (4)°) and the $[Ni([18]\text{-}aneS_6)]^{2+}$ complex.[37] The remaining six-membered chelate bite angle is larger by 4.6° (93.8 (1)°), indicating the relief of strain in the six-membered chelate ring. A facial tridentate complexation of ligand **4** requires a conformation in which all of the ligating atoms are syn endodentate. The conformations that meet this requirement are [2323], [2233],

(37) Huheey, J. E. *Inorganic Chemistry-Principles of Structure and Reactivity*, 3rd ed.; Harper and Row: New York, 1983; p 73.

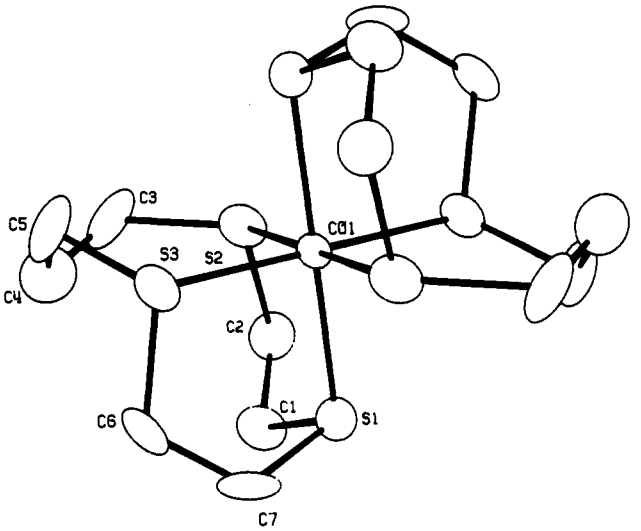


**Figure 2.** ORTEP diagram of $[Co(4)_2](ClO_4)_2$ with 25% thermal ellipsoids.

**Table V.** Selected Bond Lengths (Å) and Bond Angles (deg) for $[Co([10]\text{-}aneS_3)_2](ClO_4)_2 \cdot 2CH_3NO_2$[a]

| | | | |
|---|---|---|---|
| S(1)–Co(1) | 2.320 (3) | S(2)–Co(1) | 2.395 (3) |
| S(3)–Co(1) | 2.257 (3) | C(1)–S(1) | 1.845 (11) |
| C(7)–S(1) | 1.830 (1) | C(3′)–S(1) | 1.830 (1) |
| C(2)–S(2) | 1.809 (12) | C(3)–S(2) | 1.830 (1) |
| C(7′)–S(2) | 1.830 (1) | C(5)–S(3) | 1.830 (1) |
| C(6)–S(3) | 1.830 (1) | C(5′)–S(3) | 1.830 (1) |
| C(6′)–S(3) | 1.830 (1) | | |
| S(2)–Co(1)–S(1) | 88.0 (1) | S(3)–Co(1)–S(2) | 94.4 (1) |
| S(3)–Co(1)–S(1) | 91.5 (1) | | |

[a] Estimated standard deviations are given in parentheses.

[1333], and [1324].[30] The conformation of the complexed ligand is [2233] for the complex under study.

The molecular structure of the cobalt complex with the atomic labeling scheme is shown in Figure 2, while the fractional atomic coordinates, bond lengths, and bond angles are contained in Tables IV and V. The asymmetric unit consists of a half-molecule of the complex cation with one perchlorate anion and one molecule of nitromethane. As in the corresponding nickel complex, the three S atoms from each ligand coordinate with the Co(II) ion in a facial manner to yield an octahedral complex. The structure is centrosymmetric with the Co(II) ion occupying an inversion center resulting in a mesomeric structure.

The carbon atoms in the propyl ring (C(3), C(4), C(5)) and the ethyl ring (C(6), C(7)) were disordered, and the site occupation factors for these carbon atoms were varied similar to that of the isomorphous Ni complex. The Co–S bond lengths are slightly shorter than the Ni–S bond lengths in the Ni(II) complex of **4** (Tables III and V). Ni(II) has an ionic radius of 0.830 Å, which is intermediate between that of high-spin and low-spin Co(II) (0.885 and 0.790 Å, respectively).[37] The shorter Co–S bond length is consistent with a low-spin state in the present Co(II) complex. The observed M–S bond lengths in the series increase in the order Fe[28,29] < Co < Ni, the order of the ionic radii of the low-spin divalent ions. The Co–S distances in the present complex all differ slightly (Table V) and cannot be distinguished completely as equatorial or axial bonds. The unique bond length of 2.395 (3) Å (greater than the calculated sum of covalent radii (2.360 Å) suggests that the complex is essentially axially elongated. Moreover, the equatorial bond lengths are unequal (2.257 (3) and 2.320 (3) Å), resulting in a distorted octahedral complex in the solid state. However, in the $[Co([9]\text{-}aneS_3)_2]^{2+}$ complex ion,[1] while the axial bonds are compressed from the sum of the calculated covalent radii 2.36 Å to 2.240 (7) Å, the equatorial bonds are close to the calculated value (2.356 (6)–2.367 (5) Å). In the $[Co([18]\text{-}aneS_6)]^{2+}$ complex ion the Co–S axial bond length is elongated (2.479 (1) Å) and the equatorial bond lengths are 2.251 (1) and 2.292 (1) Å.[21] The latter species has been shown to exhibit Jahn–Teller distortion with an ESR spectrum consistent with the unpaired electron in a $d_{z^2}$ orbital. From an examination of the sum of the Co–S bond lengths, it appears that the ion under investigation is in a more distorted conformation, with the Co–S bond lengths intermediate between those of the $[Co([9]\text{-}aneS_3)_2]^{2+}$ and $[Co([18]\text{-}aneS_6)]^{2+}$ ions.

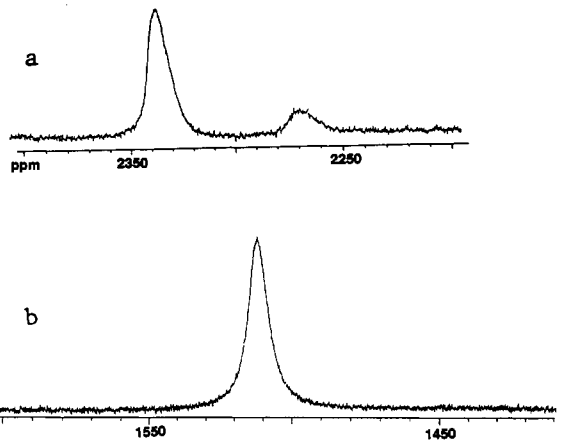


**Figure 3.** (a) $^{59}Co$ NMR spectrum of $[Co(4)_2](ClO_4)_3$ in $CH_3CN$. (b) $^{59}Co$ NMR spectrum of $[Co(1)_2](ClO_4)_3$ in $D_2O$.

The five-membered chelate ring bite angle S–Co–S was found to be 89.8 (20)°, slightly larger than the average S–Co–S angle in the $[Co([9]\text{-}aneS_3)_2]^{2+}$ complex cation (89.0 (2)°). The six-membered chelate ring angle S–Co–S was found to be 94.4 (1)° as expected. The conformation adopted by the ligand in the complex is [2233].

**NMR Spectra. $^1H$ and $^{13}C$ NMR Spectra.** The $^1H$ NMR spectrum of the Co(III) complex ion is complicated owing to the asymmetry of the ten-membered ring and also to the existence of both cis and trans isomers. The $^{13}C$ NMR spectrum of Co(III) complex ion shows seven lines at δ 17.0, 26.8, 29.2, 39.5, 40.6, 41.0, and 41.2, and they are attributed to the presence of the cis isomer in solution ($C_2$ symmetry). The spectrum is consistent with the peak at δ 17.0 being attributed to C–$CH_2$–C of the propylene bridge and those at δ 26.8 and 29.2 to the magnetically inequivalent C atoms of the propylene bridge, adjacent to the S atom. The remaining four peaks are due to the C atoms of the ethylene bridges. The conformations of the five-membered chelate rings interchange rapidly in solution, and the $^{13}C$ NMR spectra reflect the average conformations. A similar seven-line $^{13}C$ NMR spectrum has been obtained for the cis isomer of the triaza $[Co([10]\text{-}aneN_3)_2]^{3+}$ ion.[38] The peaks at δ 31.0 and 42.0 may be attributed to small amounts of the trans isomer. In general, the peaks are broad due to possible coupling with the Co nucleus ($I = {}^7/_2$). No attempt was made to separate the cis and trans isomers.

**$^{59}Co$ NMR Spectra.** The $^{59}Co$ NMR spectra of $Co([9]\text{-}aneS_3)_2(ClO_4)_3$ and $Co([10]\text{-}aneS_3)_2(ClO_4)_3$ are shown in Figure 3a,b, respectively. The spectrum of the Co complex based on **1** shows one single resonance at 1511 ppm and is in good agreement with the value of 1502 ppm obtained by Kuppers et al.[22b] For the ion $[Co(4)_2]^{3+}$ two peaks are shown at 2336 and 2268 ppm in intensity ratio 6:1, due to the presence of cis and trans isomers, respectively. The $^{59}Co$ NMR line widths depend on the electrostatic field gradients in the complexes. The electric field gradient for the cis isomer is usually smaller than that for the trans isomer.[39] A quadrupolar mechanism is the predominant mode of relaxation in Co(III) complexes devoid of full octahedral symmetry. As a result the $^{59}Co$ NMR line width for the trans isomer is broader than that for the cis isomer. This is observed in Figure 3b. The full width at half-maximum (fwhm) for the peak centered at 2336 ppm is 624 Hz and for that centered at 2268 ppm is 1220 Hz.

(38) Searle, G. H.; Angley, M. E. *Inorg. Chim. Acta* **1981**, *49*, 185.
(39) Laszlo, P. *NMR of newly accessible nuclei*; Laszlo, P., Ed.; Academic Press Inc.: New York, 1983; Vol. 2.

**Table VI.** Electronic Spectra for the Co and Ni Complexes

| complex | $\lambda_{max}$, nm ($\epsilon$, $M^{-1}$ $cm^{-1}$) | $10Dq$, $cm^{-1}$ | $B$, $cm^{-1}$ | $\beta$ | ref |
|---|---|---|---|---|---|
| $[Co(4)_2]^{2+}$ [a] | 764 (25), 565 (sh), 483 (133), 364, 284 | 13089 | | | PW[a] |
| $[Co(4)_2]^{2+}$ | 510 (sh, 370), 290 (11800) | | | | 30 |
| $[Co(1)_2]^{2+}$ | 730 (11), 560 (sh), 480 (92), 338 (6600), 264 (6500) | 13500 | | | 43 |
| $[Co(4)_2]^{3+}$ [a] | 493 (398), 374 (sh, 10247), 356 (13077), 295 (6004) | 21900 | 404 | 0.37 | PW |
| $[Ni(4)_2]^{2+}$ [a] | 824 (32), 530 (36) | 12136 | 736 | 0.71 | PW |
| $[Ni(4)_2]^{2+}$ | 807 (33), 544 (54) | 12390 | 656 | 0.63 | 30 |
| $[Ni(4)_2]^{3+}$ [b] | 567, 411, 346, 306, 283 | 17637 | | | PW |

[a] In acetonitrile. [b] Oxidized with aquocobalt(III) in perchloric acid. PW = present work.

**Electronic Spectra.** Details of the spectra of the various complexes together with the ligand field parameters are listed in Table VI. The UV–visible spectra of $[Co([10]\text{-}aneS_3)_2](ClO_4)_2$ in $CH_3CN$ show three bands at 764 (25), 565 (sh), and 483 (133) nm similar to those for the $[Co(II)([9]\text{-}aneS_3)_2^{2+}$ ion reported previously.[2] However they differ from those provided for the [10]-$aneS_3$ species measured in nitromethane.[30] The features are assigned to the $^2aT_{1g} \leftarrow {}^2A_{1g}$, $^2aT_{2g} \leftarrow {}^2A_{1g}$, and $^2bT_{2g} \leftarrow {}^2A_{1g}$ transitions, respectively. The assignments are comparable with other low-spin $d^7$ Co(II) complexes.[40-42] The ligand field strength $10Dq$, obtained from the $^2aT_{1g} \leftarrow {}^2A_{1g}$ transition, was found to be 13089 $cm^{-1}$. This value is comparable to that obtained for the low-spin $Co(1)_2^{2+}$ (13500 $cm^{-1}$).[42]

The 493-nm band in the spectrum of $[Co(4)_2](ClO_4)_3$ (Table VI) is assigned to the $^1T_{1g} \leftarrow {}^1A_{1g}$ transition. The shoulder at 374 nm could be assigned to the $^1T_{2g} \leftarrow {}^1A_{1g}$ transition. The higher value may be due to intensity "stealing" from the nearby charge-transfer band at 356 nm. Using eqs 1 and 2, and assuming $C = 4B$, the ligand field strength, $10Dq$, was found to be 21900 $cm^{-1}$ and $B = 404$ $cm^{-1}$. The nephelauxetic ratio $\beta$ for the Co(III) complex ion was found to be 0.37 ($B_0 = 1100$ $cm^{-1}$).[43]

$$E(^1T_{1g} \leftarrow {}^1A_{1g}): \quad 10Dq - C + 86B^2/10Dq = 18450 \text{ cm}^{-1} \tag{1}$$

$$E(^1T_{2g} \leftarrow {}^1A_{1g}): \quad 10Dq + 16B - C + 2B^2/10Dq = 24450 \text{ cm}^{-1} \tag{2}$$

The electronic spectrum of $[Ni([10]\text{-}aneS_3)_2](ClO_4)_2$ shows transitions due to $^3T_{2g} \leftarrow {}^3A_{2g}$ (12136 $cm^{-1}$, $\nu_1$) and $^3T_{1g}(F) \leftarrow {}^3A_{2g}$ (18519 $cm^{-1}$, $\nu_2$). These transitions involve excitation of an electron from a $t_{2g}$ to an $e_g$ orbital, e.g., $t_{2g}^6e_g^2 \rightarrow t_{2g}^5e_g^3$. The band due to $^3T_1(P) \leftarrow {}^3A_{2g}$ is obscured by a charge-transfer band. The Racah parameter for the spin-allowed transition, $B_{35}$, has been calculated from

$$B_{35} = \frac{(2\nu_1^2 + \nu_2^2 - 3\nu_1\nu_2)}{15\nu_2 - 27\nu_1} = 736 \text{ cm}^{-1} \tag{3}$$

For the free ion, $B = 1038$ $cm^{-1}$ and the nephelauxetic ratio $\beta_{35}$ for the complex has been found to be 0.71.

**Correlation of the Co Chemical Shift with d–d Electronic Transitions.** There exists a linear relation between the $^{59}Co$ chemical shift and the energy of the first optical transition in Co(III) complexes.[44,45]

Experimentally excellent correlations have been obtained between the $^{59}Co$ chemical shift and the $^1T_{1g} \leftarrow {}^1A_{1g}$ transition.[46,47]

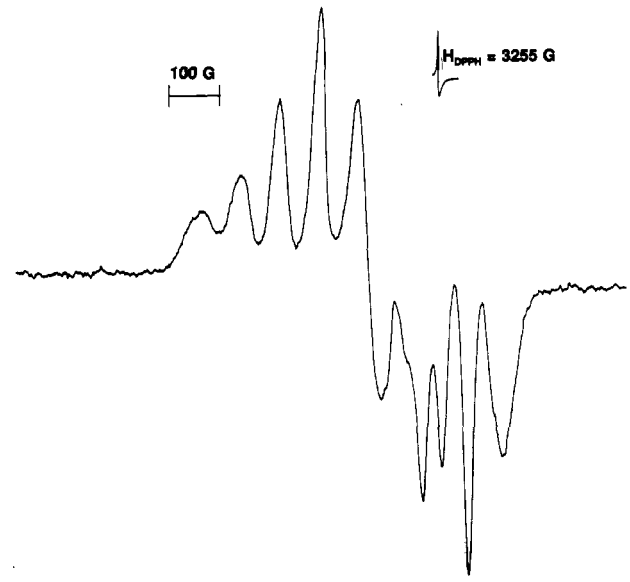


**Figure 4.** EPR spectrum of $[Co(4)_2](ClO_4)_2$ in $CH_3CN$ at 77 K.

A typical correlation plot for Co complexes containing S-ligating atoms is given in ref 46. For the $Co([10]\text{-}aneS_3)_2^{3+}$ complex the $^1T_{1g} \leftarrow {}^1A_{1g}$ transition occurs at 480 nm. The value of the $^{59}Co$ magnetogyric ratio calculated from the plot is 10.146 MHz·$T^{-1}$. This matches well with the experimental value of 10.130 MHz·$T^{-1}$ obtained from the $^{59}Co$ NMR spectrum (Figure 3b). Similarly, for the $Co([9]\text{-}aneS_3)_2^{3+}$ complex the $^1T_{1g} \leftarrow {}^1A_{1g}$ transition occurs at 476 nm. This corresponds to 10.134 MHz·$T^{-1}$ for the magnetogyric ratio of $^{59}Co$ and compares well with the experimental value of 10.121 MHz·$T^{-1}$ (from Figure 3a). Thus, for a given set of ligating atoms, using the linear plot, the $^{59}$ Co chemical shift can be predicted if the energy of the first electronic transition is known for the complex and vice versa.

**EPR Spectra.** The EPR spectrum of $[Co([10]\text{-}aneS_3)_2]^{2+}$ in $CH_3CN$ at 77 K is shown in Figure 4. The spectrum is characteristic of a low-spin $d^7$ ion in a distorted octahedral geometry. The ground state of low-spin Co(II) is $^2E_g$, which is unstable toward Jahn–Teller distortions. Axial compression would cause the unpaired electron to be in the $d_{x^2-y^2}$ orbital, and axial elongation would cause the unpaired electron to be in the $d_{z^2}$ orbital. The symmetry may be further lowered due to the asymmetry of the ten-membered ring. The crystal structure of ion $[Co([10]\text{-}aneS_3)_2]^{2+}$ shows three unequal Co–S bond lengths: 2.257 (3), 2.320 (3), and 2.395 (3) Å. The unique bond length of 2.395 (3) Å (greater than the calculated sum of covalent radii of 2.360 Å) suggests that the complex is essentially axially elongated and equatorially compressed. However, the equatorial bond lengths are unequal, giving rise to an overall rhombic distortion in the complex. Owing to the intense hyperfine structure ($^{59}Co$, $I = {}^7/_2$) the $g$ anisotropy in the $g_\perp$ feature of the ESR spectrum of the frozen sample (Figure 4) was not discernible. Thus, $g_\parallel = 2.067$, $g_\perp = 2.138$, $A_\parallel = 60$ G, and $A_\perp = 80$ G. The $[Co([18]\text{-}aneS_6)]^{2+}$ complex cation is also axially elongated with an axial Co–S bond length of 2.479 (1) Å and equatorial Co–S bond lengths of 2.251 (1) and 2.292 (1) Å.[37] The ESR spectrum is axial with $g_\parallel \sim 2$ and $g_\perp = 2.09$.[37] The variable-temperture EPR solution and powder spectra of the $[Co(1)_2](ClO_4)_2$ are characteristic of a low-spin $d_{z^2}$ ground state[18,43] with an axially elongated spectrum at 4.2 K. The Co–S bond lengths in that complex result from a dynamically averaged process at higher temperatures. The crystal structure of the $[Co(1)_2](BF_4)_2 \cdot 2CH_3NO_2$ is axially compressed with an axial Co–S bond length of 2.240 (7) Å. The axially elongated solution spectrum and the axially compressed solid-state structure is, therefore, indicative of a "planar dynamic"

(40) Backers, G.; Reinen, D. *Z. Anorg. Allg. Chem.* **1975**, *418*, 217.
(41) Kremer, S.; Henke, W.; Reinen, D. *Inorg. Chem.* **1982**, *21*, 3013.
(42) Reinen, D.; Ozarowski, A.; Jakob, B.; Pebler, J.; Stratemeier, H.; Wieghardt, K.; Tolksdorf, I. *Inorg. Chem.* **1987**, *26*, 4010.
(43) Lever, A. B. P. *Inorganic Electronic Spectroscopy*; Elsevier Publishing Co.: New York, 1968.
(44) Freeman, R.; Murray, G. R.; Richardson, R. E. *Proc. R. Soc. London, Ser. A* **1957**, *242*, 455.
(45) Ramsey, N. F. *Phys. Rev.* **1950**, *77*, 567.
(46) Jurania, N. *Inorg. Chem.* **1983**, *22*, 521.
(47) Bramley, R.; Brorson, M.; Sargeson, A. M.; Schäffer, C. E. *J. Am. Chem. Soc.* **1985**, *107*, 2780.
(48) Wieghardt, K.; Walz, W.; Nuber, B.; Weiss, J.; Ozarowski, A.; Stratemeier, H.; Reinen, D. *Inorg. Chem.* **1986**, *25*, 1651.

effect.[42] In the present study both the solid-state structure and the frozen-solution spectrum are characteristic of an axially elongated Co(II) species. The room-temperature ESR spectrum of the $[Co([10]\text{-aneS}_3)_2]^{2+}$ (present study, supplementary material) shows eight lines due to hyperfine interaction with $^{59}Co$ nucleus $I = {}^7/_2$, $A_{iso} = 40$ G, and $g_{iso} = 2.083$.

For the $g$ values of an elongated octahedron[49]

$$g_{\parallel} = g_0 + 2(\zeta^2/\delta^2) \quad (4)$$

$$g_{\perp} = g_0 + 3\zeta[(1.38/E_3) + (0.62/E_4)] + 2(\zeta^2/\delta^2) \quad (5)$$

Here, $\zeta$ is the effective spin–orbit coupling parameter and $E_3$ and $E_4$ are the transitions from $^2A_{1g}$ to the octahedral $^2aT_{2g}$ and $^2bT_{2g}$ parent states. Taking $E_3 = 17\,699$ cm$^{-1}$ and $E_4 = 20\,704$ cm$^{-1}$, from the observed $g$ values of the frozen solution spectrum $\delta$ (the energy separation between the low-spin ground-state $^2A_{1g}$ and the first excited high-spin state) was estimated to be 1218 cm$^{-1}$ and $\zeta = 219$ cm$^{-1}$. Using this value of $\delta$, the Jahn–Teller splitting energy, $4E_{JT}$, of the low-spin $^2E_g$ ground state (7502 cm$^{-1}$) can be estimated from the following equation:[42]

$$-\delta(D_{4h}) \approx 4B + 4C - \Delta - 2E_{JT} \quad (6)$$

A reasonable choice for $B$ is 730 cm$^{-1}$ by comparison with Ni(II) complexes of triaza and trithia ligands; $C = 4.35B$.[43]

The covalency parameter $K$, determined from[42]

$$\zeta = K^2\zeta_0 \quad (\zeta_0 = 540 \text{ cm}^{-1}) \quad (7)$$

was found to be 0.6, consistent with the greater covalency of the Co–S bond than the Co–N bond.

**Redox Studies. Chemical Oxidation.** Oxidation of the $[Ni([10]\text{-aneS}_3)_2]^{2+}$ cation in $CH_3CN$ using $NO^+$ gives a yellow-orange Ni(III) species, the frozen solution of which showed an ESR spectrum with $g_{xx} = 2.091$, $g_{yy} = 2.041$, and $g_{zz} = 2.022$, characteristic of a low-spin Ni(III) $d^7$ ion in a distorted octahedral environment. Similar spectra are obtained in $HClO_4$ using $PbO_2$, $Co(H_2O)_6^{3+}$, or $[Fe([9]\text{-aneS}_3)_2]^{3+}$ as an oxidant. The sequence $g_{xx}, g_{yy} > g_{zz} > g_e$ suggests that the unpaired electron is in the $d_{z^2}$ orbital ($^2A_{1g}$ ground state). The EPR spectrum is characteristic of a rhombic distortion in the Ni(III) complex, consistent with the Jahn–Teller splitting of the $^2E_g$ state and the asymmetry of the ten-membered ring.

The EPR spectrum of $[Ni([9]\text{-aneS}_3)_2]^{3+}$ ion obtained by the oxidation of the corresponding Ni(II) complex using $NO^+$ in $CH_3CN$ or $Co^{3+}$ in aqueous solutions is anisotropic with $g_{xx} = 2.076$, $g_{yy} = 2.054$, and $g_{zz} = 2.016$. Similar ESR spectra have been reported for the $[Ni([10]\text{-aneN}_3)_2]^{3+}$ ion.[49]

The UV–visible spectrum of the $[Ni([10]\text{-aneS}_3)_2]^{3+}$ ion (Table VI) shows four bands at 567, 411, 346, and 306 nm, which are tentatively assigned to the transitions $_a{}^2T_{1g} \leftarrow {}^2A_{1g}$, $_a{}^2T_{2g} \leftarrow {}^2A_{1g}$, $_b{}^2T_{1g} \leftarrow {}^2A_{1g}$, and $_b{}^2T_{2g} \leftarrow {}^2A_{1g}$, respectively. The $10Dq$ value was calculated to be 17 637 cm$^{-1}$ by comparison with similar complexes.[41,42,48] Using eqs 4 and 5 and taking $E_3$ and $E_4$ to be 24 331 and 32 680 cm$^{-1}$, respectively, $\delta$ was estimated to be 2882 cm$^{-1}$ and $\zeta = 239$ cm$^{-1}$. The covalency parameter $K$ was found to be 0.6 as against a value of 0.8[48] obtained for the $[Ni(\mathbf{2})_2]^{3+}$ complex ion and is consistent with the greater covalency of the Ni–S bond relative to that of the Ni–N bond.

**Chemical Reduction.** Reduction of $[Ni([10]\text{-aneS}_3)_2]^{2+}$ in $CH_3OH$ or $CH_3CN$ with $NaBH_4$ yields an ESR-active Ni(I) species. The ESR spectrum in $CH_3OH$ is anisotropic with $g_{xx} = 2.016$, $g_{yy} = 2.118$, and $g_{zz} = 2.207$, characteristic of a $d^9$ complex ion. The Ni(I) species so formed is stable in the absence of oxygen. In this case, the geometry around the Ni(I) ion may be an elongated octahedron with the unpaired electron in the $d_{x^2-y^2}$ orbital. The spectrum is consistent with the presence of $[Ni([10]\text{-aneS}_3)_2]^+$ in solution.

Mixed coordination environments are known to stabilize Ni(I) species against disproportionation, and monomeric Ni(I) species have been isolated.[50,51] Addition of $PPh_3$ to $CH_3CN$ solutions of the Ni(I) complex of $[10]\text{-aneS}_3$ containing $NaBH_4$ yielded a deep yellow solution with an ESR spectrum as shown in Figure 5 with a near-isotropic $g$ value of 2.157. Hyperfine interaction is evident on the high-field component ($g = 2.011$) with the multiplet arising from the coupling of one N atom ($I = 1$) from the $CH_3CN$ solvent and one P atom ($I = {}^1/_2$) from the $PPh_3$ molecule. The coupling constants were found to be ~40 and ~60 G, respectively. Although a six-line pattern is expected, owing to the similarity of the coupling constants of N and P atoms only a four-line pattern is observed. The Ni(I) ion is probably tetrahedral, with displacement of one of the trithia ligands and of one of the S donors in the other ring to yield a $NiS_2PN$ coordination sphere.

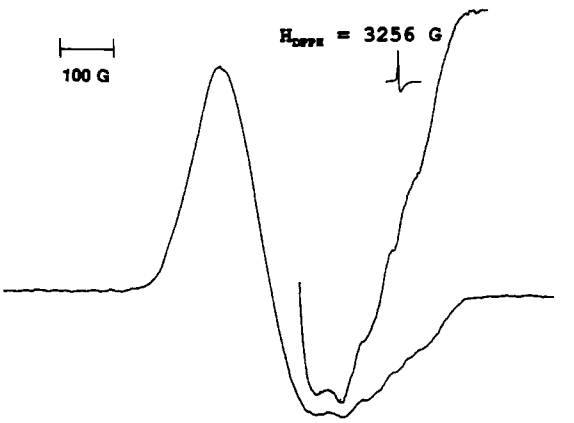


Figure 5. ESR spectrum of the Ni(I) complex cation of **4** containing $PPh_3$ at 77 K.

Table VII. Redox Potentials of the Complexes

| complex | $E_{1/2}$ (vs $Fc^+/Fc$), V | $\Delta E$, mV | $E_{1/2}$ (vs NHE), V |
|---|---|---|---|
| $[Co(\mathbf{4})_2]^{3+/2+}$ | 0.01 | 94 | 0.41 |
| $[Co(\mathbf{4})_2]^{2+/+}$ | −0.85 | 58 | −0.45 |
| $[Co(\mathbf{4})_2]^{3+/2+}$ | 0.23[b] | 112 | 0.43 |
| $[Co(\mathbf{1})_2]^{3+/2+}$ | | | 0.42[d] |
| $[Co(\mathbf{2})_2]^{3+/2+}$ | | | −0.41[e] |
| $[Co(\mathbf{4})_2]^{2+/+}$ | −0.65[b] | 118 | −0.45 |
| $[Co(\mathbf{1})_2]^{2+/+}$ | | | −0.48 |
| $[Ni(\mathbf{4})_2]^{3+/2+}$ | 0.90 | 78 | 1.30 |
| $[Ni(\mathbf{4})_2]^{2+/+}$ | −1.00 | 170 | −0.60 |
| $[Ni(\mathbf{4})_2]^{2+/+}$ | −0.95[c] | 171 | −0.55 |

[a] In 1 M $CF_3SO_3H$, $E_{1/2}$ vs Ag/AgCl. [b] In 1 M $NaNO_3$, $E_{1/2}$ vs saturated calomel electrode (SCE). [c] $Ag^+/Ag$ (0.1 M $AgNO_3$) reference electrode, $E_{1/2}$ vs $Fc^+/Fc$. [d] Reference 21. [e] Reference 53.

Reduction of $[Ni([9]\text{-aneS}_3)_2](ClO_4)_2$ electrochemically or chemically using $NaBH_4$ in acetonitrile under an inert atmosphere yielded a pale yellow Ni(I) species. Frozen (77 K) solutions of this species yielded an ESR spectrum with a near-isotropic $g$ value of 2.135, since the $g_{\parallel}$ and $g_{\perp}$ features are not fully resolved. Addition of $PPh_3$ produced a deep yellow species, which is also ESR active with a near-isotropic $g$ value of 2.164. Hyperfine interaction is seen on the high-field region similar to that of the Ni(I) complex ion of $[10]\text{-aneS}_3$ and is consistent with a $NiS_2PN$ coordination sphere.

The formation of a detectable Ni(I) complex ion reflects the ability of the soft S atoms in stabilizing the soft Ni(I) ion. The presence of a mixed coordination environment containing softer P atoms also helps to stabilize the Ni(I) ion. The S donor atoms in thioether ligands can thus act as $\pi$ acceptors using empty d orbitals on the S atoms thereby stabilizing low oxidation states, as is confirmed by the formation of the ESR-active Ni(I) complexes.

(49) Fairbank, M. G.; McAuley, A.; Norman, P. R.; Olubuyide, O. *Can. J. Chem.* **1985**, *63*, 2983.
(50) McAuley, A.; Subramanian, S. *Inorg. Chem.* **1990**, *29*, 2830.
(51) Bontempelli, G.; Magno, F.; Corain, B.; Schiavon, G. *Inorg. Chem.* **1981**, *19*, 99.
(52) Wieghardt, K.; Schmidt, W.; Herrmann, W.; Kuppers, H.-J. *Inorg. Chem.* **1983**, *22*, 2953.

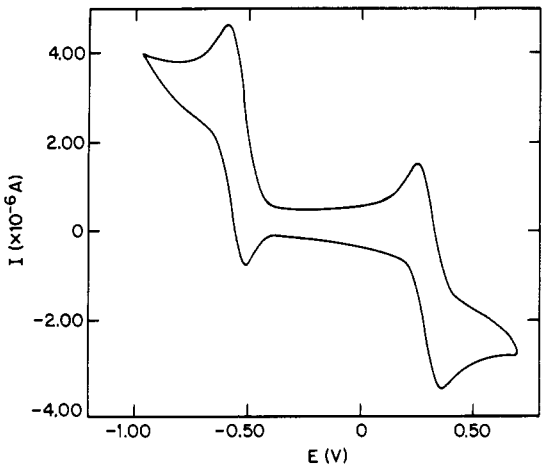


**Figure 6.** Cyclic voltammogram of $[Co(4)_2](ClO_4)_2$ in $CH_3CN$ containing 0.1 M $NEt_4BF_4$.

**Electrochemistry.** Electrochemical data for the $[Co(4)_2]^{2+}$ ion together with related crown thioether complexes are summarized in Table VII. Electrochemical studies on $[Co(4)_2]^{2+}$ in $CH_3CN$ showed two redox waves with $E_{1/2}$ = 0.41 V (vs NHE) attributed to the $[Co(4)_2]^{3+/2+}$ couple and −0.45 V (vs NHE) due to the $[Co(4)_2]^{2+/+}$ couple (Figure 6). The $[Co(4)_2]^{2+/+}$ couple is reversible with a peak to peak separation of 58 mV. In aqueous solutions two quasi-reversible waves were obtained at 0.43 and −0.45 V for the corresponding redox couples. The $E_{1/2}$ values are similar to those obtained for the $[Co(1)_2]^{3+/2+}$ and $[Co(1)_2]^{2+/+}$ couples (Table VII). The redox potential of the $[Co(4)_2]^{2+/+}$ couple moves slightly to more positive values relative to the $[Co(1)_2]^{2+/+}$ couple based on the nine-membered ligand **1** and is also reversible in $CH_3CN$ solutions. The larger trithia ligand **4** together with the softer S atoms thus stabilizes the soft Co(I) ion. In comparison with the Co complexes of triaza ligands the redox potentials of the $Co^{3+/2+}$ couple based on trithia ligands are much more positive. The difference between the $E_{1/2}$ values of the $[Co(4)_2]^{3+/2+}$ couple and the $[Co(2)_2]^{3+/2+}$ couple[53] is 840 mV. This again reflects the ability of the softer S atoms to stabilize the Co(II) ion, whereas the N ligands stabilize the Co(III) state.

Electrochemical studies on the $[Ni(4)_2]^{2+}$ complex ion in $CH_3CN$ (using a Ag wire as the reference electrode and ferrocene as the external standard) showed two quasi-reversible redox couples, one at 0.90 V (vs $Fc^+/Fc$, $\Delta E$ = 78 mV), due to the $[Ni(4)_2]^{3+/2+}$ couple. A reduction wave was also observed at −1.00 V (vs $Fc^+/Fc$, $\Delta E$ = 170 mV), due to the $[Ni(4)_2]^{2+/+}$ couple. In a different experiment, when $Ag/AgNO_3$ (0.1 M) was used as a reference electrode in $CH_3CN$, a quasi-reversible redox wave was obtained at −0.95 V vs $Fc^+/Fc$ ($\Delta E$ = 171 mV) due to $[Ni(4)_2]^{2+/+}$ and another irreversible wave was seen at 0.0 V vs $Fc^+/Fc$. Upon adding $PPh_3$, the oxidation peak at 0.0 V disappeared and a more reversible wave at −1.08 V (vs $Fc^+/Fc$), $\Delta E$ = 70 mV, was obtained. This suggests a stabilization of the Ni(I) complex, which may be a distorted octahedral species or a tetrahedral species containing sulfur atoms from trithia ligands and a phosphorus atom of the $PPh_3$ molecule.

**Electron-Transfer Reactions.** In the present study, the NMR line-broadening technique has been used to measure directly the electron-transfer rates of the transition-metal complexes. The oxidation of the $[Co(4)_2]^{2+}$ ion involves the electronic configurational change of $[core](t_{2g}^6e_g^*) \rightarrow [core](t_{2g}^6)$, i.e., removal of an electron from an antibonding $e_g$ orbital. Since the electron transfer occurs between low-spin Co(II) and low-spin Co(III) complex ions, there is no contribution from the barrier due to the spin change as is often the case in Co complexes with aza ligands. All these factors make the $Co(S_6)^{3+/2+}$ system ideal for the study of electron-transfer reactions.

(53) Macartney, D. H. Presented at the 72nd Canadian Chemical Conference and Exhibition, Victoria, BC, Canada, June, 1989; Paper INOR 265.

**Table VIII.** Dependence of the Spectral Line Widths (Fwhm) of the $[Co(4)_2]^{3+}$ Ion[a] and $[Co(1)_2]^{3+}$ Ion[b] on the Concentrations of the Corresponding Paramagnetic Co(II) Complex Ions

| spectrum no. | $[Co(4)_2]^{2+}$ mM | fwhm, Hz | $[Co(1)_2]^{2+}$, mM | fwhm, Hz |
|---|---|---|---|---|
| 1 | 0.00 | 996 | 1.04 | 611 |
| 2 | 0.70 | 1033 | 1.93 | 644 |
| 3 | 1.40 | 1173 | 3.20 | 679 |
| 4 | 1.84 | 1191 | 4.54 | 752 |
| 5 | 2.49 | 1317 | 7.32 | 870 |
| 6 | 3.16 | 1428 | 8.21 | 913 |
| 7 | 3.78 | 1478 | | |

[a] 1.5 mM [Co(III)]; $I$ = 0.2 M $[N(C_2H_5)_4BF_4]$; 75% $CH_3CN$, 25% $CD_3CN$; $T$ = 303 K. [b] 1.3 mM [Co(III)]; $I$ = 0.1 M ($NaNO_3$); $D_2O$; $T$ = 303 K.

The electron-transfer barriers in $[Co([9]\text{-}aneS_3)_2]^{3+/2+}$ and $[Co([9]\text{-}aneN_3)_2]^{3+/2+}$ have been measured and analyzed in the frame of the Marcus–Sutin model.[23,24] The Marcus analysis depends on the availability of self-exchange rate data for the reagents used in these studies. Recently,[22b,53] the self-exchange rate constant for the $[Co(1)_2]^{3+/2+}$ couple was determined using $^1H$ NMR line-broadening techniques. The $^1H$ NMR spectrum of the corresponding $[Co(4)_2]^{3+}$ ion is dense and complicated due to the asymmetry of the ten-membered ring. As a result, the $^1H$ NMR line-broadened spectra are poorly resolved, making linewidth measurements difficult. On the other hand, the simplicity and the sensitivity of the $^{59}Co$ NMR spectrum renders it apt to be used as a probe for the study of outer-sphere electron-transfer reactions. The rate constant of the self-exchange reaction

$$[Co^*(4)_2]^{3+} + [Co(4)_2]^{2+} \rightleftarrows [Co(4)_2]^{3+} + [Co^*(4)_2]^{2+} \quad (8)$$

in $CH_3CN$ was determined using the $^{59}Co$ NMR line-broadening technique. The $^{59}Co$ NMR spectrum of the $[Co(4)_2]^{3+}$ ion showed one intense line at 2336 ppm (cis isomer) and another relatively broad and weak line at 2268 ppm (trans isomer). Addition of the paramagnetic $[Co(4)_2](ClO_4)_2$ complex to $CH_3CN$ solutions of the diamagnetic $[Co(4)_2]^{3+}$ ion at ambient temperatures ($T$ = 25 ± 1 °C) resulted in additional broadening of the Co(III) resonance line (Figure 7 and Table VIII). The line width of the $^{59}Co$ NMR resonance at $\delta$ 2336 is plotted against the concentration of the paramagnetic Co(II) species in Figure 8. From the slope of the plot the self-exchange rate constant $k_{11}$ for reaction 8 was determined as follows: In the slow-exchange region

$$k_{11} = \frac{\pi\{\text{fwhm (Hz)}\}}{[\text{Co(II)}]\ (\text{M})} = \pi(\text{slope})\ (\text{M}^{-1}\ \text{s}^{-1})$$
$$= 4.3 \times 10^5\ \text{M}^{-1}\ \text{s}^{-1} \quad (9)$$

Although the temperature dependence of the line broadening was not monitored, the line broadening was assumed to be in the slow-exchange regime.[25] The assumption is reasonable considering the fact that the line broadening was found to be independent of the concentration of the diamagnetic species. The value of 4.3 × $10^5$ $M^{-1}$ $s^{-1}$ for $k_{11}$ is about 6 orders of magnitude higher than that obtained for the $Co(N_6)$ systems, e.g., $[Co(2)_2]^{3+/2+}$ (8 × $10^{-2}$ $M^{-1}$ $s^{-1}$).[22] The electron transfer in the amine system, $[Co(2)_2]^{3+/2+}$, involves change from the high-spin $Co^{2+}$ to the low-spin $Co^{3+}$ ion. As a result, the Co–N bond distances in both the reduced and the oxidized forms are very different.[22] In the thia systems, e.g., $[Co(4)_2]^{3+/2+}$ both the Co(III) and the Co(II) ions are in the low-spin state resulting in a very small change in the Co–S bond distances in the two oxidation states. The smaller inner-sphere reorganization energy leads to larger self-exchange rate constant for the $Co(S_6)$ systems. It is of interest that a value of 1.6 × $10^5$ $M^{-1}$ $s^{-1}$ (25 °C, $I$ = 0.2 M) has been obtained[22b] for the $[Co(1)_2]^{3+/2+}$ exchange, very similar to the present number. However, the rate is about 50 times faster than that observed by Osvath and Sargeson[54] (2.8 × $10^4$ $M^{-1}$ $s^{-1}$, 27 °C, $I$ = 0.10 M)

(54) Osvath, P.; Sargeson, A. M.; Skelton, B. W.; White, A. H. *J. Chem. Soc., Chem. Commun.* **1991**, 1036.

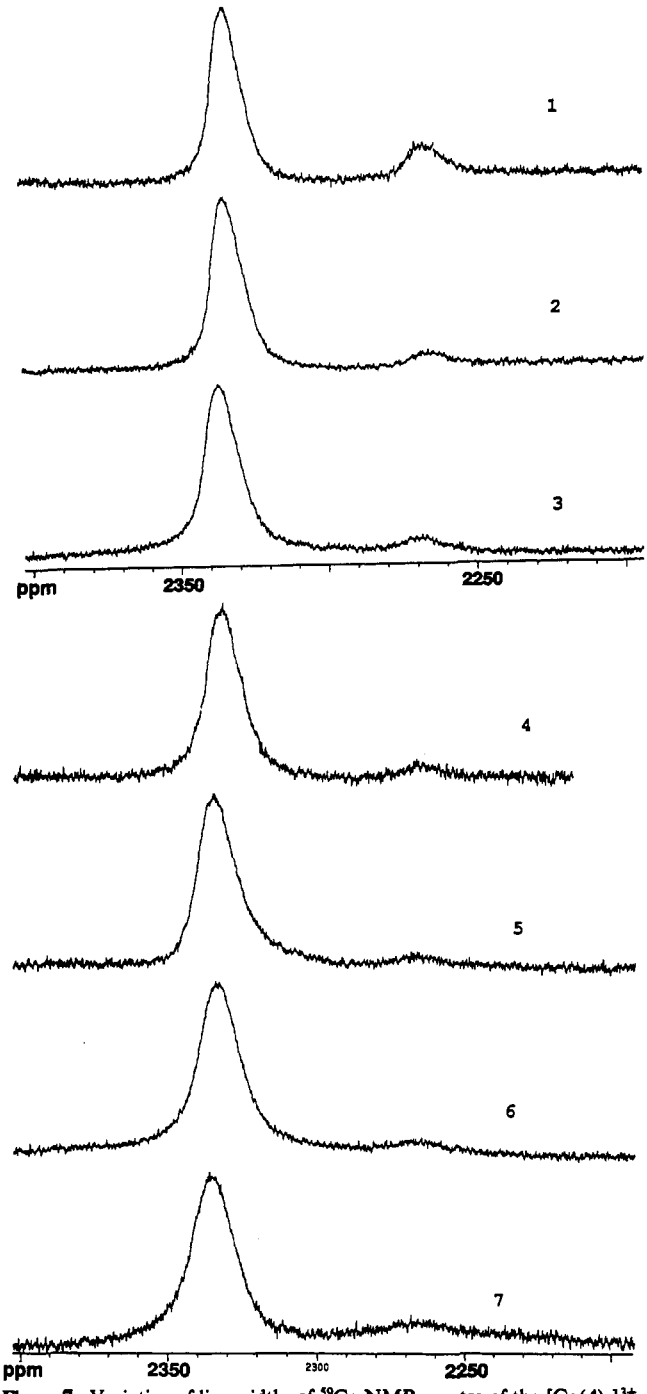


Figure 7. Variation of line widths of $^{59}Co$ NMR spectra of the $[Co(4)_2]^{3+}$ ion with the concentration of the paramagnetic $[Co(4)_2]^{2+}$ ion.

in the reactions of a hexathioether cage. The latter value is closer to that derived by Dubs et al.[27] in their study of electron-transfer reactions between low-spin $Co^{II}$- and $Co^{III}(S_3N_3)$ cage complexes, where the electron-transfer self-exchange rate was also measured by the $^1H$ NMR line-broadening technique and was found to be $4.5 \times 10^3$ $M^{-1}$ $s^{-1}$ but again significantly larger (4 orders of magnitude) than the corresponding $Co(N_6)$ systems.

The self-exchange rate constant for the reaction

$$[Co^*(1)_2]^{3+} + [Co(1)_2]^{2+} \rightleftarrows [Co(1)_2]^{3+} + [Co^*(1)_2]^{2+} \quad (10)$$

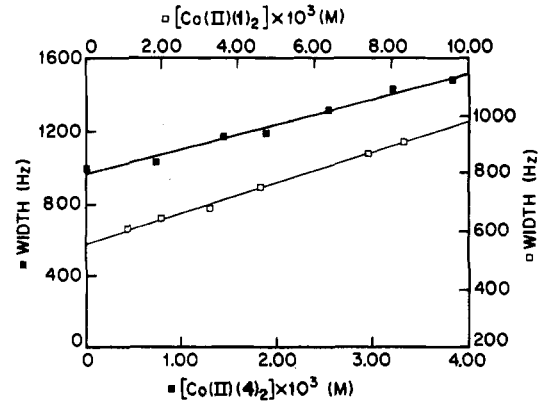


Figure 8. Plots of $^{59}Co$ NMR line widths of the $[Co(4)_2]^{3+}$ ion and $[Co(1)_2]^{3+}$ ion vs the concentration of the corresponding paramagnetic Co(II) complex ions.

was also determined using the $^{59}Co$ NMR line-broadening technique by use of the single peak at $\delta$ 1511. Addition of paramagnetic $[Co(1)_2]^{2+}$ ion resulted in an increase of the diamagnetic line width (Table VIII). From the plot of the line width vs the paramagnetic Co(II) concentration, (Figure 8), the self-exchange rate constant for reaction 10 was found to be $1.3 \times 10^5$ $M^{-1}$ $s^{-1}$. This value compares well with the rate constant obtained from the $^1H$ NMR line-broadening measurements, $1 \times 10^5$ $M^{-1}$ $s^{-1}$,[53] and is in excellent agreement with that obtained independently by Wieghardt ($1.6 \times 10^5$ $M^{-1}$ $s^{-1}$).[22b] On the basis of the force constants for the Co–S bonds in reaction 10, the self-exchange rate constant was calculated using the Marcus–Sutin model and was found to be $1 \times 10^6$ $M^{-1}$ $s^{-1}$.[22a] The self-exchange rate constant obtained for the $[Co(1)_2]^{3+/2+}$ couple in the present study agrees reasonably well with the predicted value. The similarity of the self-exchange rate constant for the $[Co(4)_2]^{3+/2+}$ couple in $CH_3CN$ and the $[Co(1)_2]^{3+/2+}$ couple in water suggests that the contribution to the outer-sphere reorganization barrier due to solvation effects is small.

Thus, the knowledge of the self-exchange rate constant for the $Co^{3+/2+}$ redox couple based on the trithia ligand 4 would permit the complex to be used as an one-electron outer-sphere reagent in electron-transfer reactions in nonaqueous solutions.

**Acknowledgment.** We thank the Natural Sciences and Engineering Research Council (NSERC) of Canada for support. The assistance of Ms. Christine Greenwood in the NMR experiments and of Ms. Kathy Beveridge in the single-crystal studies is gratefully acknowledged.

**Registry No.** $[Co(1)_2](ClO_4)_3$, 102573-49-9; $[Ni(1)(CH_3CN)(PPh_3)]^+$, 137824-11-4; *trans*-$[Co(4)_2](ClO_4)_2$, 137894-42-9; *trans*-$[Co(4)_2](ClO_4)_3$, 137824-08-9; *trans*-$[Co(4)_2](ClO_4)_2 \cdot 2CH_3NO_2$, 137894-45-2; *trans*-$[Co(4)_2]^+$, 137824-12-5; *cis*-$[Co(4)_2]^{3+}$, 137894-46-3; *trans*-$[Ni(4)_2](ClO_4)_2$, 137894-44-1; *trans*-$[Ni(4)_2](ClO_4)_3 \cdot 2CH_3NO_2$, 137939-45-8; *trans*-$[Ni(4)_2]^{3+}$, 137824-09-0; *trans*-$[Ni(4)_2]^+$, 137824-10-3; $[Ni(4)(CH_3CN)(PPh_3)]^+$, 137824-13-6.

**Supplementary Material Available:** Tables S1–S10, containing experimental crystallographic data, anisotropic temperature parameters, bond lengths, bond angles, and intermolecular distances for the Ni and Co complexes, and Figures S1 and S2, showing a room-temperature ESR spectrum of the Co(II) complex ion and an ESR spectrum of the Ni(I) complex ion of [9]-ane$S_3$ in $CH_3CN$ containing $PPh_3$ at 77 K (13 pages); Tables S11 and S12, listing calculated and observed structure factors (15 pages). Ordering information is given on any current masthead page.